

This is a repository copy of *Acoustic modeling using the digital waveguide mesh*.

White Rose Research Online URL for this paper:

<https://eprints.whiterose.ac.uk/3708/>

---

**Article:**

Murphy, Damian [orcid.org/0000-0002-6676-9459](https://orcid.org/0000-0002-6676-9459), Kelloniemi, Antti, Mullen, Jack et al. (1 more author) (2007) *Acoustic modeling using the digital waveguide mesh*. IEEE Signal Processing Magazine. pp. 55-66. ISSN 1053-5888

<https://doi.org/10.1109/MSP.2007.323264>

---

**Reuse**

Items deposited in White Rose Research Online are protected by copyright, with all rights reserved unless indicated otherwise. They may be downloaded and/or printed for private study, or other acts as permitted by national copyright laws. The publisher or other rights holders may allow further reproduction and re-use of the full text version. This is indicated by the licence information on the White Rose Research Online record for the item.

**Takedown**

If you consider content in White Rose Research Online to be in breach of UK law, please notify us by emailing [eprints@whiterose.ac.uk](mailto:eprints@whiterose.ac.uk) including the URL of the record and the reason for the withdrawal request.

*promoting access to White Rose research papers*



**Universities of Leeds, Sheffield and York**  
**<http://eprints.whiterose.ac.uk/>**

---

White Rose Research Online URL for this paper:  
<http://eprints.whiterose.ac.uk/3708/>

---

**Published paper**

Murphy, D., Kelloniemi, A., Mullen, J. and Shelley, S. (2007) *Acoustic Modeling Using the Digital Waveguide Mesh*, IEEE Signal Processing Magazine, Volume 24 (2), 55 - 66.

---



# Acoustic Modeling Using the Digital Waveguide Mesh

Recent activities in articulatory vocal tract modeling, room impulse response synthesis, and reverberation simulation

**T**he digital waveguide mesh (DWM) is a numerical simulation technique based on the definition of a regular spatial sampling grid for a particular problem domain, which in this specific case is a vibrating object capable of supporting acoustic wave propagation resulting in sound output. It is based on a simple and intuitive premise—the latter often considered important by the computer musicians who are the primary users of a sound synthesis algorithm—yet the emergent behavior is complex, natural, and capable of high-quality sound generation. Hence, the DWM has been applied in many areas of computer music research since it was first introduced by Van Duyne and Smith in 1993 [1]. This article is the first to attempt to consolidate and summarize this work. The interested reader is also directed to [2], where DWM modeling is considered in the more general

context of discrete-time physics-based modeling for sound synthesis, and [3], where the DWM is examined within a rigorous theoretical and comparative framework for more established yet related wave scattering numerical simulation techniques.

## THE ONE-DIMENSIONAL DIGITAL WAVEGUIDE

The one-dimensional (1-D) digital waveguide is based on a time and space discretization of the d'Alembert solution to the 1-D wave equation. This approach to sound synthesis was first used in the Kelly-Lochbaum model of the human vocal tract for speech synthesis [4] and has parallels with other, more generally applied wave variable scattering modeling paradigms such as the transmission line matrix (TLM) method [5] and wave digital filters (WDFs) [6]. However it was Julius O. Smith III who first proposed the term *digital waveguide* and used these techniques

initially for artificial reverberation [7] and later for sound synthesis [8], [9]. Digital waveguides have remained the most popular and successful physical modeling-based sound synthesis technique to date, due to the realistic, high-quality sounds that can be generated, often in real-time and so therefore also facilitating effective user interaction. This research has also been made more widely accessible through a range of commercially available physical modeling hardware synthesizers developed by Yamaha in the early 1990s based on digital waveguide techniques [10]. The reader is referred to [9] and [11] for a thorough treatment and discussion of this area and a full derivation of some of the equations that are introduced in what follows. Consider the 1-D wave equation for transverse motion with speed  $c$  on an ideal, infinitely long, vibrating string:

$$\frac{\partial^2 y(t, x)}{\partial t^2} = c^2 \frac{\partial^2 y(t, x)}{\partial x^2}. \quad (1)$$

The d'Alembert or traveling wave solution to (1) is defined as:

$$y(t, x) = y^+(t - x/c) + y^-(t + x/c), \quad (2)$$

where  $y^+$  and  $y^-$  are arbitrary twice-differentiable functions denoting wave movement to the left and right, respectively. Assuming that  $y^+$  and  $y^-$  are bandlimited to half the sampling rate of the system allows the discrete time version of (2) to be defined for spatial sampling points  $mX$  and sampling interval  $nT$  such that  $X = cT$ :

$$y(nT, mX) = y^+(n - m) + y^-(n + m). \quad (3)$$

This solution can be implemented in an efficient and straightforward manner using two parallel digital delay lines to represent the left-going and right-going traveling wave components. Figure 1 shows a digital waveguide implementation of an ideal string, rigidly terminated at either end of the  $M$ -sample delay lines, corresponding to the nut and bridge of a typical instrument. The system is excited with an appropriate input "loaded" into the upper and lower delay lines at position  $x_{in} = m_{in}cT$  and a physical output is obtained at  $x_{out} = m_{out}cT$  by sum-

ming the upper and lower values according to (3), being exact at the sampling points of the system.

### THE SCATTERING JUNCTION

The terminations introduced in the 1-D string shown in Figure 1 are a special case of signal scattering. An input signal will propagate without loss until it is incident upon a change in system impedance, resulting in transmission and/or reflection of the incident signal. This example leads to the formal definition for a lossless scattering junction, now given without loss of generality in terms of acoustic pressure rather than string displacement. At such a junction, system continuity must be preserved in terms of pressures and volume velocities analogous to Kirchhoff's Laws for parallel connection of electrical circuit elements. Assuming  $N$  connected waveguide elements with the pressure in each defined as  $p_i$  and volume velocities as  $u_i$ , then for lossless scattering the following must hold:

$$p_1 = p_2 = \dots = p_i = \dots = p_N = p_J, \quad (4)$$

$$u_1 = u_2 = \dots = u_i = \dots = u_N = 0 \quad (5)$$

Note that  $p_J$  is defined as the actual pressure value at the point of connection for these  $N$  waveguide elements, referred to as the pressure value at scattering junction  $J$ . Scattering junctions, together with the 1-D waveguide elements described above, provide the basic building blocks for a digital waveguide physical model of a vibrating system. For instance, six 1-D strings could be coupled together via a scattering junction to simulate the bridge of a guitar, facilitating sympathetic resonances where excitation on one string causes low-amplitude oscillation on one or more of the others due to energy transmitted through the bridge. Similarly, this scattering junction could also allow coupling to a filter to simulate the effects of body resonances. Hence, scattering junctions also act as system sampling points where physical variables may be tapped off for coupling with other aspects of the model or with the outside world. Similarly, they can also be used to allow energy to be input to a system. In modeling a wind instrument such as a clarinet, the bore can be implemented as a 1-D lossless waveguide coupled with the more

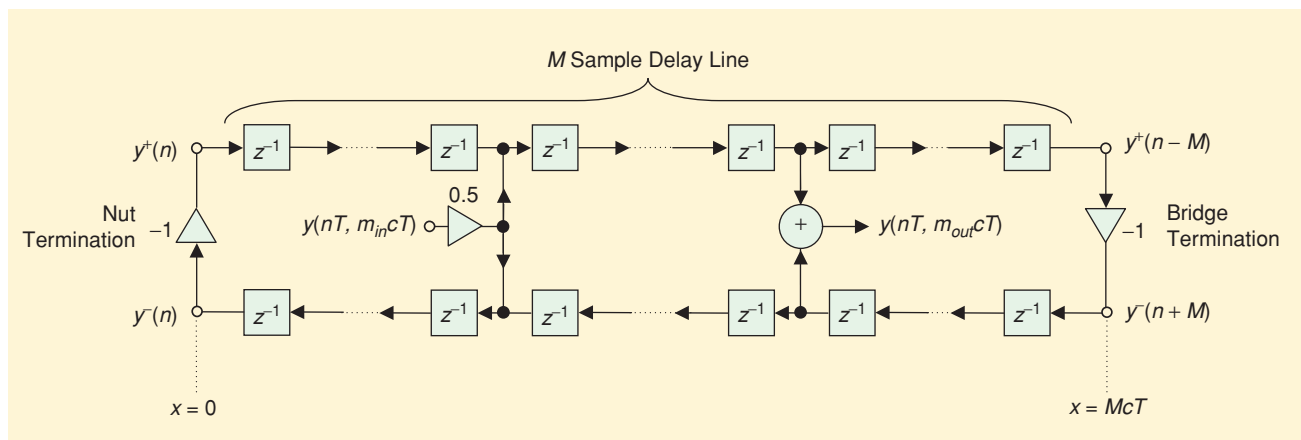


**[FIG1]** The ideal lossless 1-D digital waveguide string model, which is  $M$ -samples long and rigidly terminated at either end.

complex, nonlinear breath pressure/reed input function via an appropriate scattering junction implementation [9].

Figure 2(a) shows the functional block diagram for a general lossless scattering junction  $J$  with  $N$  neighbors, with each connected unit waveguide element having an associated admittance  $Y_i$ . The impedance of a waveguide is given by  $Z_i = p_i/u_i$  and hence the admittance  $Y_i = 1/Z_i$ . The signal  $p_{J,i}^+$  represents the *incoming* signal to junction  $J$  along the waveguide from the opposite junction  $i$ . Similarly, the signal  $p_{J,i}^-$  represents the *outgoing* signal from junction  $J$  along the waveguide to the opposite junction  $i$ . Connecting delay lines together at scattering junctions in a more general sense allows spatial and temporal sampling grids to be defined and gives rise to families of models that are more generally known as digital waveguide networks (DWNs). The Kelly-Lochbaum vocal tract model and the simply terminated 1-D string as shown in Figure 1 are both examples of specific DWNs. A DWN with a more complex arrangement of multiport interconnections can be used to simulate reverberation, as in the first application of digital waveguides [7] and more recently explored in [12]. However a DWN consisting of (typically) unit delay waveguide elements and  $N$ -port lossless scattering junctions conforming to a regularly arranged and spaced grid structure gives rise to a particular family of two- or three-dimensional (2-D or 3-D) structures. These are called *digital waveguide meshes* and are more directly analogous in construction to the physical objects they are attempting to simulate.

### THE DIGITAL WAVEGUIDE MESH

The DWM was first proposed by Van Duyne and Smith [1] as an extension to 1-D digital waveguide sound synthesis appropriate for modeling plates and membranes, potentially leading to full 3-D object modeling. Acoustic wave propagation through a DWM is determined according to the scattering equations and associated mesh topology. For a lossless junction  $J$  according to conditions (4) and (5) or directly from Figure 2(a), the sound pressure  $p_J$  at junction  $J$  for  $N$  connected waveguides can be expressed as:

$$p_J = \frac{2 \sum_{i=1}^N Y_i \cdot p_{J,i}^+}{\sum_{i=1}^N Y_i}. \quad (6)$$

Noting from (3) that the total sound pressure  $p_J$  in a waveguide element connected to junction  $J$  can also be defined as the sum of the traveling waves in this element, or alternatively as the sum of the input and output gives:

$$p_J = p_{J,i}^+ + p_{J,i}^- \quad (7)$$

And finally, as the waveguide elements in a DWM are equivalent to bi-directional unit-delay lines, the input to scattering junction  $J$  at time index  $n$ ,  $p_{J,i}^+(n)$  is equal to the output from neighboring junction  $i$  into the connecting waveguide at the

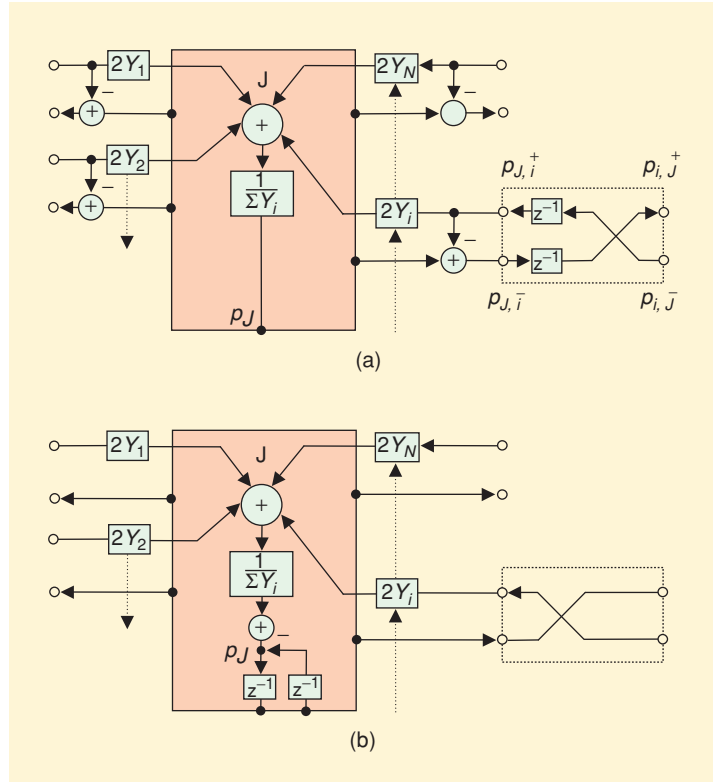


**[FIG2] Functional block diagrams for the general lossless scattering junction  $J$  with  $N$  neighbors: (a) the W-model case and (b) the K-model case. Note that in each example a single connecting waveguide element has been connected to terminal  $Y_i$ .**

previous time step,  $p_{i,J}^-(n-1)$ . Expressing this relationship in the  $z$ -domain gives:

$$p_{J,i}^+ = z^{-1} \cdot p_{i,J}^- \quad (8)$$

Hence, from (6) junction pressure values are calculated according to input values from immediate neighbors, output values are calculated using (7) and then propagated to neighbors via the bi-directional waveguide elements, becoming inputs at the next iteration according to (8). From (6), (7), and (8) via an appropriate linear transformation it is possible to derive an equivalent formulation in terms of junction pressure values only:

$$p_J = \frac{2 \sum_{i=1}^N Y_i \cdot p_i \cdot z^{-1}}{\sum_{i=1}^N Y_i} - p_J \cdot z^{-2}. \quad (9)$$

Expression (9) can also be derived directly from a finite difference time domain (FDTD) formulation of the 2-D case of the wave equation in (1). The functional block diagram for the scattering junction implementation described by (9), equivalent to Figure 2(a), is shown in Figure 2(b). Digital waveguide models represent signal propagation via two directional wave components and schemes implemented in this way, according to (6), (7) and (8), are termed *W-models* or *W-DWDMs* [2], [13], [14]. A linear transformation of a W-DWM leads to this alternative implementation as a Kirchhoff variable DWM (K-DWM) [2],

[13], [14], as given in (9), and depending on physical quantities only rather than sampled traveling-wave components. In this form, and under certain conditions, a K-DWM can be computationally equivalent to a FDTD simulation.

Mixed modeling scenarios where K-DWM and W-DWM approaches have been interfaced in 1-D via a *KW-pipe* have been proposed in [14], [15], leading to the formulation of a 2-D hybrid DWM [13], [16], [17]. The 2-D hybrid mesh combines the computational efficiency of the K-DWM approach in terms of computation time and memory use, with the flexibility of scattering-based boundary termination options for complex geometries through the use of KW-pipes. Typically, KW-hybrid DWMs demonstrate a speed up in processing time of the order of 34% with a 50% decrease in use of main system memory [16]. A K-DWM scattering junction connected to a W-DWM scattering junction via a KW-pipe is shown in Figure 3.

The W-DWM or K-DWM scattering equations can be used to implement a range of topologies/structures. In 2-D the most commonly implemented topologies are the four-port rectilinear and six-port triangular mesh structures shown in Figure 4(a) and (b). A thorough comparison of their relative characteristics, together with those of the three-port hexagonal mesh, is presented in [18]. Two-dimensional DWM models based on the rectilinear or triangular topology have been most commonly used for synthesis of percussion instruments such as plates, membranes, and gongs [19]–[21], as well as for 2-D reverberation modeling [22]. Three-dimensional topologies as shown in

Figure 4(c)–(f) include the rectilinear [23]; tetrahedral [24], [25]; dodecahedral [also known as cubic close packed (CCP)] [26]; and octahedral structures, and a similar analysis of their characteristics is presented in [27].

Three-dimensional DWM structures are applied to a range of sound synthesis applications. The work of [28] combines a 2-D triangular mesh model of a drum membrane coupled to a 3-D rectilinear model of a drum-shell to give a more complete model of a percussion instrument. DWM models have been applied to simulate 3-D resonant objects [26], [29], [30], sometimes in combination or parallel with other digital waveguide models; for instance, to provide synthesis of complex instrument resonances [31], [32], or to simulate a 3-D acoustic space with multiple 2-D cross-sectional simulations [33]. However, most current research activity in 3-D DWM modeling is in its application to the accurate synthesis of acoustic spaces, and this will be discussed in the Applications section.

An additional subset of K-DWMs has also been subject to much investigation and these are based on an interpolated rectilinear mesh structure in either 2-D [34] or 3-D [35]. Interpolated DWMs demonstrate wave propagation characteristics approaching that of triangular/dodecahedral topologies but without the additional overheads of a denser and more complex topological structure.

#### DWM LIMITATIONS

There are a number of important factors that impose limitations on DWM models as an optimal solution for all sound synthesis

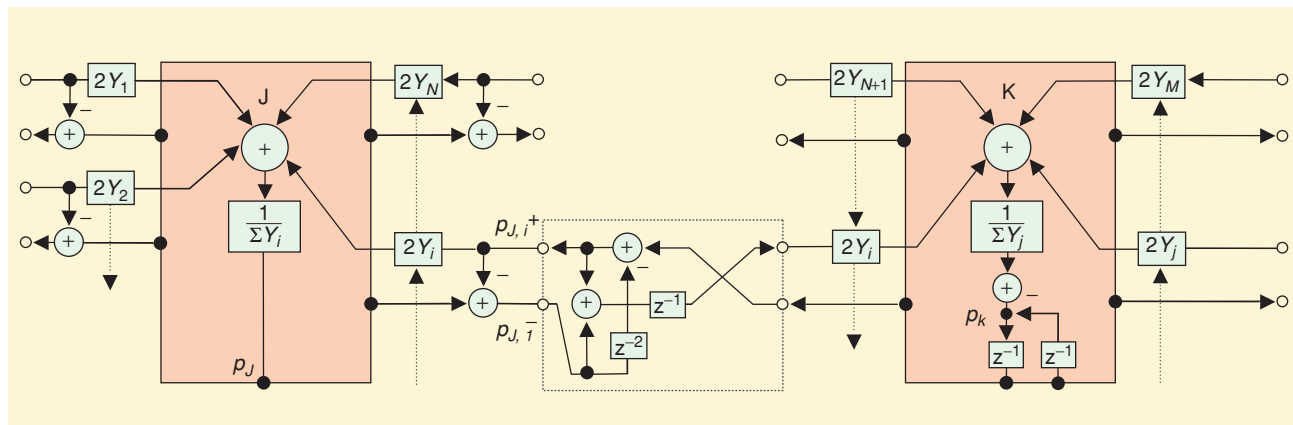


[FIG3] Functional block diagram for a W-DWM scattering junction  $J$  with  $N$  neighbors connected to a K-DWM scattering junction  $K$  via a KW-pipe connecting waveguide element.

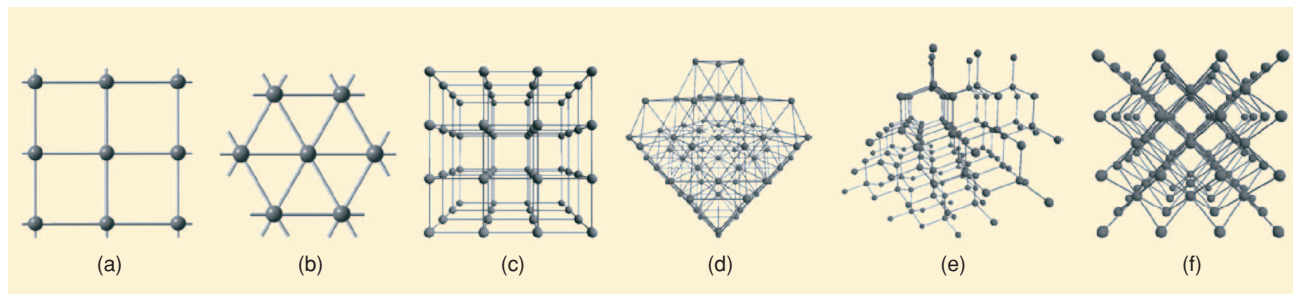


[FIG4] DWM topologies: (a) four-port 2-D rectilinear; (b) six-port 2-D triangular; (c) six-port 3-D rectilinear; (d) 12-port 3-D dodecahedral (CCP); (e) four-port 3-D tetrahedral; (f) eight-port 3-D octahedral.

applications. One of the most significant advantages of the 1-D digital waveguide that originally made it a realistic proposition for applications in sound synthesis is the computational efficiency of the approach when compared with a brute-force numerical solution to the system wave equation. This is further improved through the ability to commute losses to specific lumped points in the system, significantly reducing the number of calculations required per time-step iteration. Unfortunately, the elegance of this approach is lost when moving to higher dimensions. With a DWM-based system, acoustic wave propagation is determined by signal interaction at the scattering junctions and hence a calculation must take place at every junction for every time-step. Reducing the number of scattering junctions reduces the sample rate of the DWM and hence the effective bandwidth of the system. The advantage gained with the DWM approach, however, is in the structural immediacy of the simulation, allowing objects to be defined based only on physical and geometrical definitions, and the ability to observe and interact with the system at physically relevant or meaningful points.

A more specific DWM limitation is *dispersion error*, where the velocity of a propagating wave is dependent upon both its frequency and direction of travel, leading to wave propagation errors and a mistuning of the expected resonant modes. The degree of dispersion error is highly dependent upon mesh topology and has been investigated in, for example, [3], [18], [24], [27]. In 2-D both the interpolated and triangular DWMs demonstrate dispersion characteristics that are substantially reduced to a function of frequency only. In 3-D, minimization of dispersion can be similarly achieved through the use of interpolated or dodecahedral topologies. Appropriate pre- and postprocessing of results from these mesh structures allows offline frequency warping techniques to be used to correct mis-tuned resonances [34], [35]. Alternatively, frequency warping can be incorporated directly as part of a DWM scattering junction [36], [37]. However, although accurate synthesis of resonant modes is required for the dominant low-frequency properties of a vibrating system, dispersion error is considered less important with increasing frequency as modal density increases, and human perception of such variations becomes less critical. Oversampling a DWM can also offer improvements such that the required bandwidth lies within accepted limits, typically  $0.25 \times f_{\text{update}}$  [1], where  $f_{\text{update}}$  for a DWM of dimension  $D$  and spatial sampling distance  $d$  is generally given by:

$$f_{\text{update}} = \frac{c\sqrt{D}}{d}, \quad (10)$$

where  $c$  is the speed of sound. Ultimately  $f_{\text{update}}$  dictates the quality of audio signal output from a DWM with large sample rates requiring denser meshes, more computer memory, and hence taking longer to run, limiting even the most efficient large-scale K-DWMs to offline generation only.

### DWM BOUNDARY TERMINATION

There exist a number of possibilities for terminating a DWM at a system boundary. In [21] a  $10 \times 10$  node 2-D rectilinear DWM is

terminated with single one-pole all-pass filters, which may be interpreted as a 1-D termination connected to an ideal spring, allowing modal frequencies in the DWM to be re-tuned or corrected appropriately. For curved boundaries, where the perimeter of the structure being modeled is not normal/parallel to the axes of the mesh, noninteger length waveguide elements called *rimguides* can be used [20] and have been demonstrated as appropriate for accurate low-frequency modeling of circular membranes using a 2-D triangular mesh.

A commonly applied solution is to passively terminate a DWM using a simple 1-D connection that implements a change in admittance such that there is no signal return from the connected boundary over a finite time duration. Hence, the associated input value for such a connection in Figure 2, or using (6) or (9), is set to zero. This termination acts to reflect an incident signal according to the change in admittance of the connected waveguide elements. In the simplest case, for a one-port boundary-node  $p_B$  connected to a single  $N$ -port scattering junction  $p_1$  with a change in waveguide admittance from  $Y$  to  $Y_B$ , a reflection coefficient  $-1 \leq r \leq 1$  is determined such that:

$$r = \frac{Y - Y_B}{Y + Y_B} \quad (11)$$

and  $p_B$  can therefore be calculated as a function of the sound pressure of the incident traveling wave variable from  $p_1$ :

$$p_B = (1 + r) \cdot p_{B,1+}. \quad (12)$$

In the equivalent K-DWM case, a passive termination is equivalently implemented as a feedback loop between waveguide element terminals in Figure 2 with unit delay as derived in [13], [38] and given by

$$p_B = (1 + r)p_1 \cdot z^{-1} - r \cdot p_B \cdot z^{-2}. \quad (13)$$

Note that  $r = 1$  or  $r = -1$  gives total reflection and  $r = 0$  approximates anechoic conditions. Full derivations of boundary conditions for the general  $N$ -port boundary termination for K-, W-, and KW-hybrid cases is offered in [16] and a similar boundary implementation for a triangular DWM using multipoint reflection factors is presented in [29].

### APPLICATIONS OF THE DWM

The digital waveguide mesh in 2-D and 3-D has been applied to a diverse range of applications where simulation of acoustic wave propagation within an enclosed system is required. What follows is a summary of recent results and research in this area, namely for vocal tract synthesis, object modeling, synthesis of room impulse responses, and how this method can be extended to abstract higher dimensions.

#### 2-D VOCAL TRACT MODELING FOR SPEECH SYNTHESIS

The well-established 1-D Kelly-Lochbaum vocal tract model [4] is based on a linear series of concatenated cylindrical acoustic tubes, each of different cross-sectional area, and each tube

section implemented as a 1-D digital waveguide element. A number of developments on this basic model include nasal tract, lip radiation, and wall losses to synthesize the singing voice [39] and the use of fractional waveguides to make lengthwise changes to tract shape [40], [41]. Standard waveguide elements have also been substituted for conical equivalents using scattering methods derived from the spherical wave equation. This increases model accuracy, giving higher-order area function approximation, but adds to the computational load and introduces possible stability problems [40], [42]. More recent work has explored the possibility of replacing the basic 1-D digital waveguide implementation with a 2-D DWM model that simulates the variation in cross-sectional area along the vocal tract directly through an appropriately shaped mesh geometry [43]. Formant patterns produced using the 2-D DWM implementation are equivalent to those produced by a very high-resolution 1-D digital waveguide acoustic tube-based simulation. The 2-D model also offers simulation of cross-tract modes due to the additional dimension of freedom for acoustic oscillation and propagation and approximately linear control over formant bandwidths via the additional reflection parameter at the side walls of the vocal tract. Hence, the 2-D DWM vocal tract offers improvements similar to other developments based on enhanced-order acoustic tube area function approximation, together with additional model flexibility such as the ability to simulate a split in the air channel used in the creation of sounds such as /l/.

The disadvantages of this proposed voice synthesis mechanism rest in its inability to simulate smooth, continuous dynamic changes to the tract area functions to facilitate articulated voice synthesis, and the high mesh sample rate  $f_{\text{update}}$  required to ensure accurate tracking and mapping of vocal tract shape resulting in an implementation that can only work offline. Both of these problems have been analyzed and a solution proposed in a new implementation of the 2-D DWM [44]. In this new method, rather than mapping acoustic tube area function directly to the 2-D DWM geometry, a constant-width 2-D rectangular DWM, 17.5 cm long with  $f_{\text{update}} = 44.1$  kHz is used. The waveguide element impedance across the width of this rectangular geometry is then varied according to the

area function information. A minimum impedance channel  $Z_{\text{min}}$  is defined as the lowest value across the range of vowels to be simulated, corresponding directly to the largest cross-sectional area  $A_{\text{max}}$ , and from this a maximum tract width

opening can be defined. An *impedance map* is constructed for a particular vowel tract shape such that each area function value  $A(x)$  along the length of the tract walls corresponds to a maximum impedance value  $Z_x$ . An impedance curve varying from  $Z_x$  to  $Z_{\text{min}}$  and back to  $Z_x$  at the opposite wall is then defined across the

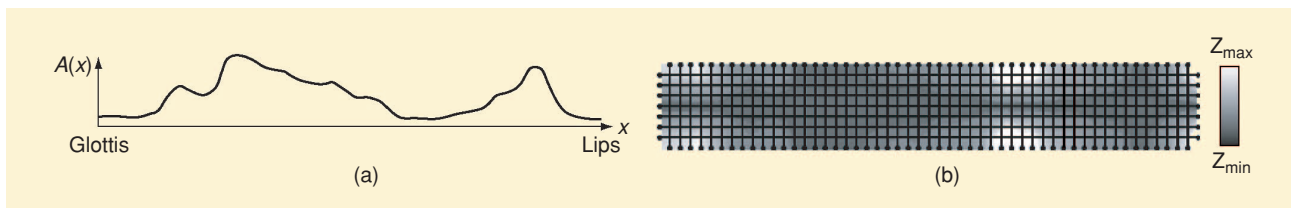
tract according to a raised cosine function, with the minimum impedance channel equidistant between the tract walls.

Figure 5(a) shows the cross-sectional area function information  $A(x)$  taken from MRI scans [45] as it varies along the length of the vocal tract from glottis to lips. Figure 5(b) is the corresponding impedance map imposed across and along the underlying rectangular 2-D DWM based on a four-port rectilinear topology. Areas of higher impedance are represented by a lighter shading, and the minimum impedance channel can be observed as the darker area along the center of the map. Figure 6(a) shows the resulting formant pattern for this vocal tract shape, when excited by a noise source at the glottis and measured at the lip end. The dotted lines have been generated from a high-resolution 1-D waveguide model, using the same area functions for comparison purposes, and measured average formant values are also shown.

Software developed to test the real-time dynamic behavior of this 2-D DWM vocal tract model is available for download and use at [47], and initial results based on this system were first presented in [44]. This application also facilitates real-time dynamic articulation. An example is presented in Figure 6(b) demonstrating a smooth linear interpolation between area function data for the /a/ (“bard”) and /e/ (“bed”) vowels under noise source excitation to highlight the resulting change in formant patterns.

Figure 6 shows that this new 2-D dynamically varying DWM demonstrates results in terms of simulated formant frequencies that are in good agreement with both a high-resolution 1-D model and real-world values. Figure 6(a) seems to indicate that the 2-D model is closer to real-world formant values than the high-resolution 1-D case, although this accuracy actually varies

**DIGITAL WAVEGUIDES HAVE REMAINED THE MOST POPULAR AND SUCCESSFUL PHYSICAL MODELING-BASED SOUND SYNTHESIS TECHNIQUE TO DATE, DUE TO THE REALISTIC, HIGH-QUALITY SOUNDS THAT CAN BE GENERATED.**



**[FIG5] Forming the impedance mapped /u/ vowel DWM: (a) cross-sectional area function; (b) rectilinear mesh with raised cosine impedance map.**



with target vowel/tract-shape and the real-world values used. In general, the two modeling methods are in good agreement with one another. Also, Figure 6(b) demonstrates a smooth transition between vocal tract shapes without any discontinuity for the 1-D and 2-D cases, being of particular importance in the latter example. Hence, from these generally comparable results the 2-D dynamically varying DWM can be seen to offer an alternative to current 1-D dynamic vocal tract models, while also offering additional advantages over these 1-D implementations as discussed above and presented in [43] for static simulations of the vocal tract. The reader is invited to test the software presented in [47] and compare the audio output from both 1-D and 2-D models under LF glottal source excitation. Informal perceptual testing has demonstrated that users consider the 2-D example to be more “natural-sounding” than the similar 1-D case.

This work is the first demonstration of a dynamically varying DWM model, in this case operating in real-time. Most prior DWM work has been based on a static representation of the acoustic system under study, partly due to the computational resources required for real-time implementation and user interaction, and partly due to possible discontinuities in the output from the resulting model. Hence, this work potentially opens new areas of research and application areas for DWM modeling, possibly moving to direct user-input and feedback that has currently only been possible in 1-D digital waveguide synthesis. Further work in this area will concentrate on developing appropriate tract wall boundary filters and facilitate lengthwise shape changes for modeling lip protrusion required for accurate synthesis of the /u/ vowel. This work also demonstrates the potential of moving toward a full 3-D DWM model using 3-D MRI scans of the vocal tract shape incorporating complex-shape cross-sectional area data.

## 2-D OBJECT MODELING

The DWM is often used to synthesize the acoustic properties of a 2-D or 3-D resonant body as these objects are a fundamental

component of most musical instruments, serving to both amplify and modify the characteristics of a source excitation. Given that the resonating aspects of most instrument bodies are relatively small implies that a high-resolution DWM implementation is feasible—in real-time in the case of the vocal tract model above—with modern computing facilities. Consider the classic example of a 2-D ideal stretched circular membrane. The resonant frequencies  $f_{mn}$  can be defined according to the nature of their *nodal regions* where  $m$  represents the number of nodal lines positioned along the *diameter* of the membrane and  $n$  represents the number of circular nodal lines, including the boundary. The fundamental frequency of an ideal membrane  $f_{01}$  can be calculated according to its physical properties (for example, as presented in [19]). Subsequent modes are fixed relative to  $f_{01}$ .

Figure 7(a) shows the nodal regions of an ideal stretched circular membrane with diameter 0.5 m, implemented using a highly oversampled 2-D triangular DWM, with  $f_{\text{update}} = 192$  kHz, resulting in a spatial sampling distance of 0.00253 m and a total of 35,742 junctions. The membrane is excited near the boundary with a lowpass-filtered impulse and an output is obtained at a junction near the opposite boundary. To model an ideal membrane with clamped edges, the reflection coefficients  $r$  at the boundary of the mesh are set to  $-1$ . The modes (0,2), (1,1), (2,1), and (3,1), are shown, with associated frequencies given relative to  $f_{01}$ . Figure 7(b) plots the spectrum of the output against the theoretical predicted frequencies for the fundamental and first nine modes.

Note that from Figure 7(b) there is an exact correlation between the predicted modal frequencies and those obtained via simulation, and this is due to the high mesh sample rate used, minimizing dispersion error effects for the bandwidth studied, and ensuring a smooth mesh fit to the circular boundary of the membrane without using rimguides.

An exciting possibility with physical modeling synthesis is that, with clear defined rules governing system behavior, it becomes relatively straightforward to extend these rules to

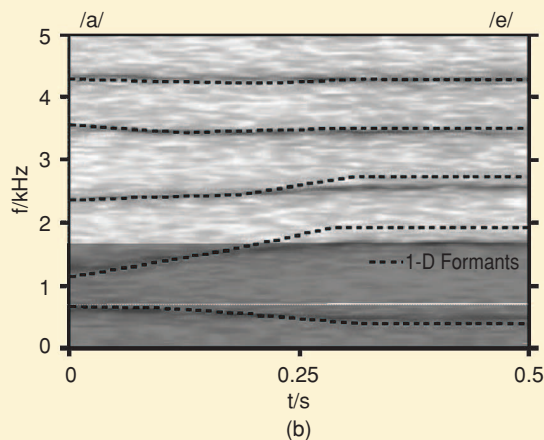
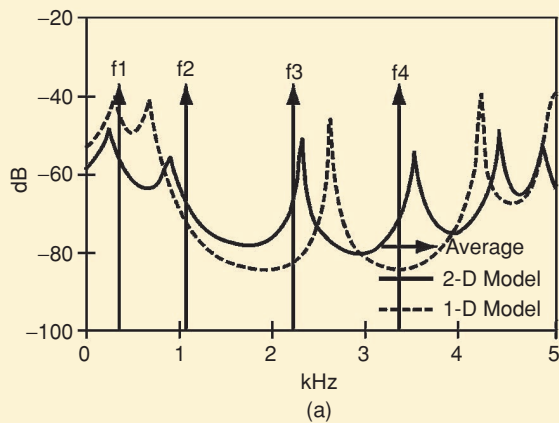


**[FIG6]** Formant patterns from the impedance-mapped DWM under noise excitation: (a) /u/ vowel compared with a high resolution 1-D model and average measured values; (b) /a/ to /e/ diphthong compared with same 1-D model.

situations that could not exist, or are difficult to control, in the real world. Figure 8 presents one such example as an extension of the 2-D circular membrane and shows the two lowest modes of resonance from a DWM membrane simulation of a tri-foil radiation symbol with diameter and  $f_{\text{update}}$  as before, this time resulting in a model consisting of 25,549 junctions. Sound examples for these simple 2-D objects are available at [48]. In isolation the sounds produced from such basic 2-D membranes, although percussive in nature, are somewhat uninspiring and require a more complete model for accurate and interesting object synthesis and, hence, these examples should be considered as a starting point only. Further research in improved modeling of resonant objects has considered DWNs for more complex theoretical multidimensional systems [3], specific

aspects such as coupling a 2-D membrane to a 3-D resonator [28], improved nonlinear excitation [49], and using simple DWM resonators to model the high-frequency characteristics of complex instrument bodies [31]. Also of note is the Sounding Object Project that has explored physical modeling, including 2-D and 3-D DWMs of resonating objects, with a view to matching the perception of synthesized sounds to the modeled objects that created them [26], [29], [50].

### SYNTHESIS OF ROOM IMPULSE RESPONSES

The first application of DWMs in the field of room acoustics simulation was by Savioja et al. in 1994 [23]. Fundamentally, synthesizing the characteristics of a bounded space using a DWM is exactly the same as synthesizing the sound of a vibrating

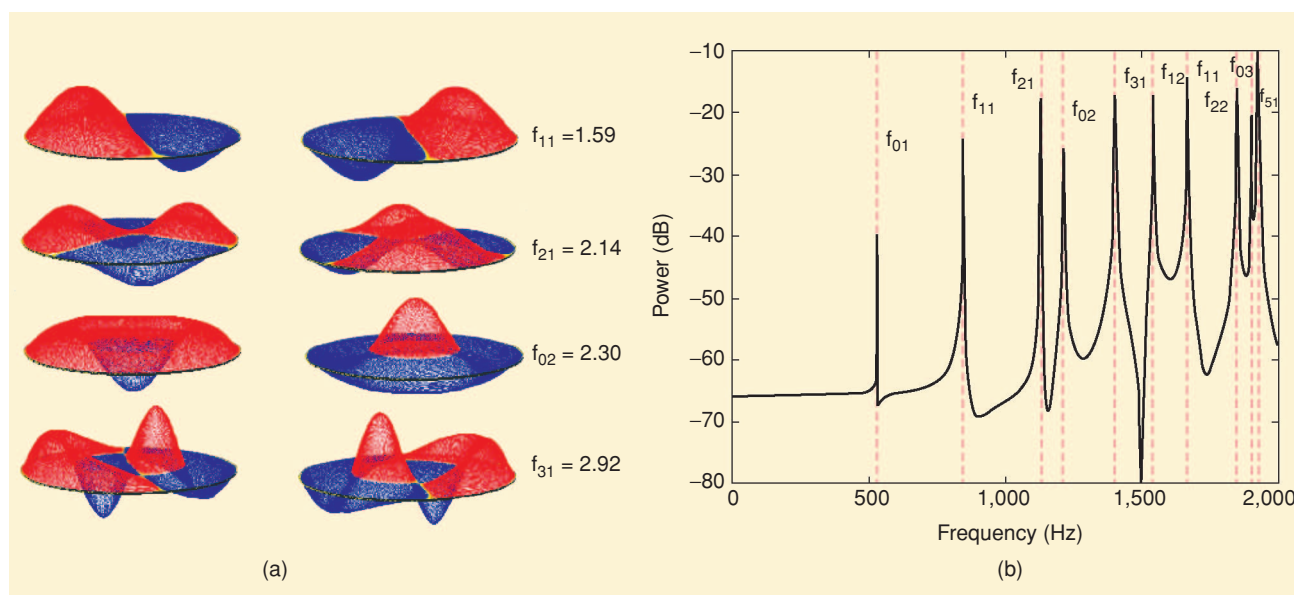


[FIG7] 2-D triangular DWM model of a membrane with a diameter of 0.5 m: (a) animation captures from the resulting simulation demonstrating resonance at modes (0,2), (1,1), (2,1), and (3,1); (b) actual output spectrum compared with predicted modal frequencies.

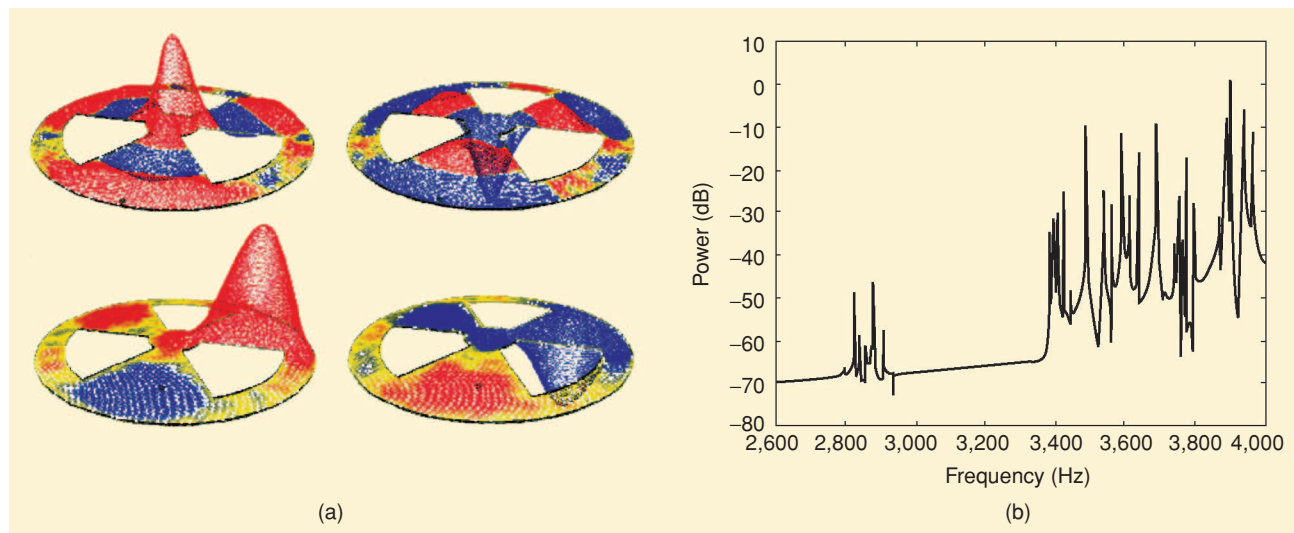


[FIG8] 2-D triangular DWM model of a physically impossible system—a trifoil radiation symbol membrane with a diameter of 0.5 m: (a) animation captures from the resulting simulation demonstrating modal resonances; (b) output spectrum.

physical object. However, in the latter example, sound output is generated directly from the modeled object by reading sample values at a scattering junction, whereas with room acoustics modeling it is a room impulse response (RIR) that is synthesized rather than the actual sound source. The RIR is generally of little interest in terms of its direct audio quality; however, when convolved with an arbitrary anechoic audio input the result is to perceive the audio source as if placed within the modeled space. Also, the relative size of the DWMs used as 3-D acoustic spaces are many times larger than, for example, the 2-D vocal tract presented above, and hence take considerably longer to execute, implying offline RIR synthesis only.

It has been shown that DWMs offer accurate RIR synthesis at low frequencies [51] and demonstrate natural wave phenomena such as interference and diffraction [52], with high-frequency accuracy being limited by  $f_{\text{update}}$  and the dispersion error of the selected topology. This contrasts with other RIR synthesis methods based on geometric acoustic techniques [53] that are typically valid for high frequencies only. Other research has explored how 3-D spaces, or their reverberant characteristics, might be simulated using 2-D models, significantly reducing computational resources [22], [33]. However, the accurate simulation of DWM boundaries is still a key research area with a view to how the physical properties of real materials might be modeled. This has included how 1-D boundary termination might be optimized for anechoic conditions [54] [55], leading to a new spatially averaged approach for the  $0 \leq r \leq 1$  case [56]. Optimized absorption/reflection across a wide range of angles of incidence for  $-1 \leq r \leq 1$  has been facilitated using the *admittance boundary* method [57], where a DWM is terminated with additional layers of boundary-nodes behind the actual boundary location, in turn terminated using an optimal anechoic solution.

For accurate simulation of real acoustic boundaries, frequency-dependent reflection/absorption must be implemented. In [58], a boundary-node is replaced with a boundary filter defined to optimally match given frequency-dependent material reflection coefficients and implemented using a first-order infinite impulse response filter for a 2-D rectilinear K-DWM. This results in a good approximation to the target response but is subject to the directional-dependent characteristics of the mesh topology, being less accurate for certain angles of incidence.

The other important characteristic of a real-world acoustic boundary is whether a reflection is *specular*, where the angle of

reflection is equal to the angle of incidence, or *diffuse* such that the incident energy is redistributed over a range of angles. Previous diffuse boundary implementations for a DWM are effective but limited, either in terms of accuracy [20], or by sacrificing user control for an optimal solution [59]. A new technique based on [20] simulates accurate diffusion with a high degree of control and consistency by rotating incoming junction signals via a circulant matrix at a *diffusing layer* of standard  $N$ -port W-DWM air-nodes adjacent to the boundary [60]. The model is lossless and allows other boundary conditions, such as frequency-dependent absorption, to be easily incorporated.

Much of this recent application-focused research has been incorporated as part of the *RoomWeaver* DWM-based room acoustics research tool first presented in [17] and shown in Figure 9. The purpose of the system is to allow the user to intuitively set up enclosed space geometry, boundary surface, and source/receiver parameters required to generate an RIR by means of a simple scripting language and graphical user interface. High-quality reverberation and auralization for a wide range of spaces/applications are possible using high-resolution 2-D triangular and 3-D mesh topologies both based on a KW-hybrid implementation. A range of RIRs synthesized according to varied initial conditions and associated audio examples are available for download [48]. For complete synthesis of a sound event it would be desirable to incorporate a 3-D dynamically variable instrument model within a larger 3-D DWM of a performance space, requiring appropriate interfacing across DWM types according to the space and instrument models used. Although nontrivial, this has been considered in the case of a drum model using a 2-D triangular DWM membrane with a 3-D rectilinear shell [28] and in the more general case [3]. However, such complete synthesis could only be offered via the offline RIR generation/real-time convolution processing paradigm due to the computational expense of full 3-D space modeling. Such examples are presented in [48] for a 2-D DWM vocal tract processed with DWM-synthesized RIRs.

#### THE HYPER-DIMENSIONAL DIGITAL WAVEGUIDE MESH

From (6) it is clear that dimensionality is not inherent in the scattering equations. For example, the four-port lossless scattering junction is the main algorithmic building block of both the 2-D rectilinear and 3-D tetrahedral mesh. The spatial arrangement of the surrounding scattering junctions—the

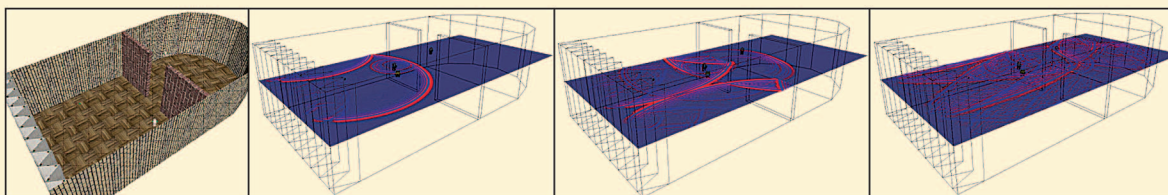


**[FIG9]** DWM room acoustics modeling in *RoomWeaver* incorporating the latest implementations of frequency-dependent and diffusive boundaries. A completely defined acoustic space followed by wave propagation snapshots through a 2-D horizontal plane of the same space viewed in wireframe mode is shown from left to right.

mesh topology—is the determining factor and it is therefore possible to extend the scattering junction concept beyond three spatial dimensions to *hyper-dimensional DWMs* [23], [61] that have been shown as appropriate for simulating artificial reverberation [62].

At low frequencies, the acoustic characteristics of a room can be modeled with sufficient accuracy by approximating the main dimensions of a basic cuboid model and simulating the corresponding resonant modes. In real rooms there are typically additional architectural features that lead to frequency-dependent irregularity in these predicted trajectory lengths. Hence, at higher frequencies, a typical RIR will demonstrate a large number of densely and irregularly distributed modal peaks that are not determined by the basic geometry of the space alone. However, for high-quality artificial reverberation not all of these modes need to be simulated directly, with approximately 1,500 modes distributed evenly or along a logarithmic scale between 80 Hz and 10 kHz being sufficient for diffuse and natural sounding artificial reverberation [63]. In a DWM, the number of primary resonant modes is equal to the number of dimensions, with higher dimensions leading to a more irregular arrangement of modal peaks. It is possible to extend these equations describing the resultant wave propagation to the hyper-dimensional case, where for each mesh dimension  $x_i$  the primary mode has a frequency corresponding to  $(c/2L_i)$  with  $L_i$  defined as the trajectory length. In an  $N$ -dimensional space, standing waves occur at the following frequencies:

$$f_{n_1 n_2 n_3 \dots n_N} = \frac{c}{2} \sqrt{\left[ \sum_{i=1}^N \left( \frac{n_i}{L_i} \right)^2 \right]}, \quad (14)$$

where  $n_i$  is the integer index of the current mode for each dimension and  $c$  is the speed of sound. Furthermore, at a specif-

ic modal frequency, the sound pressure value at a point  $(x_1, x_2, x_3, \dots, x_N)$  inside such space is determined by:

$$p_{n_1 n_2 n_3 \dots n_N}(x_1, x_2, x_3, \dots, x_N) = A \prod_{i=1}^N \cos\left(\frac{n_i x_i}{L_i}\right), \quad (15)$$

where  $A$  is an arbitrary amplitude coefficient.

Examples of modal distributions calculated using (15) are shown in Figure 10(a). Note that the additional advantage of a hyper-dimensional DWM reverb is the resultant high-density distribution of high-frequency modes while simultaneously avoiding potentially problematic (in terms of perceived sound quality) low-frequency resonances. This is due to the trajectories being kept shorter compared to a similar model with the same number of junctions but lower dimensionality and is demonstrated in Figure 10(b) comparing 2-D and four-dimensional DWMs. Hence, hyper-dimensional DWM reverb satisfies the requirement for a densely distributed high frequency modal response while giving the freedom for the more precise and sparsely arranged low-frequency modes to be modeled with any other appropriate technique without frequency overlap. Further work for a more natural reverberant effect requires the implementation of frequency-dependent losses to simulate air and boundary absorption as used in RIR synthesis with standard 2-D and 3-D DWM models.

## CONCLUSIONS

The digital waveguide mesh has been an active area of music acoustics research for over ten years. Although founded in 1-D digital waveguide modeling, the principles on which it is based are not new to researchers grounded in numerical simulation, FDTD methods, electromagnetic simulation, etc. This article has attempted to provide a considerable review of how the DWM has been applied to acoustic modeling and sound synthesis problems, including

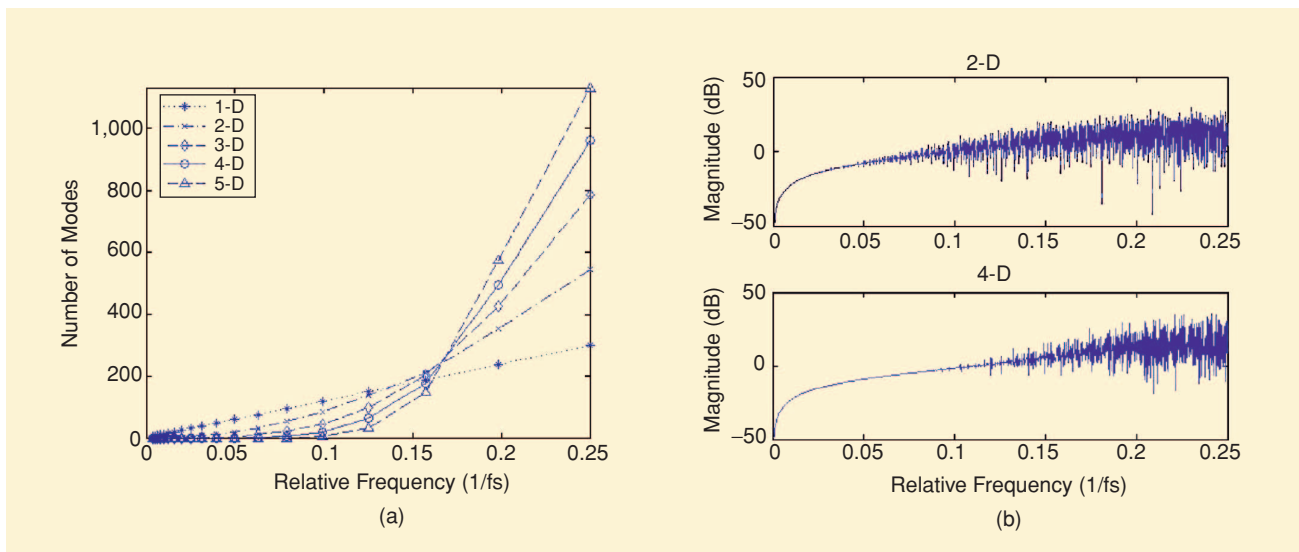


**[FIG10]** Frequency response information for 2,310 node DWMs of varying dimension: (a) theoretical modal distribution varying with increasing dimensionality; (b) frequency response of a 2-D and 4-D DWM.

new 2-D object synthesis and an overview of recent research activities in articulatory vocal tract modeling, RIR synthesis, and reverberation simulation. The extensive, although not by any means exhaustive, list of references indicates that though the DWM may have parallels in other disciplines, it still offers something new in the field of acoustic simulation and sound synthesis. Perhaps one reason for the continued interest in this area is the natural and intuitive complex emergent behavior that results from such simple, locally defined scattering equations. However, despite this perceived simplicity, it is also clear that there are still many nontrivial problems to be solved. There are few current examples of useful and playable virtual instruments using DWM based sound synthesis (although a virtual drum in the London Science Museum that can be played in real-time and is a realization of the work presented in [28] is a notable exception), and this is mainly due to the computational resources required for such a real-time model. Nonreal-time operation is not a problem when simulating static, linear time-invariant systems such as a representation of an acoustic space, and hence most recent DWM work has focused in this area. The real-time convolution of an audio input signal with the impulse response generated from such a model is trivial to implement on a modern computing platform and is now a commonly used sound processing operation. Offline, only DWM-based virtual instruments for sound synthesis prohibit user interaction and severely limit playability. However, some of the recent developments presented in this article, particularly those relating to dynamic, real-time vocal tract simulation, are beginning to make significant inroads in this area and will hopefully lead to new DWM implementations that can be applied more generally—and more successfully—to the diverse range of possible sound synthesis applications.

#### ACKNOWLEDGMENT

This work is supported in part by the U.K. Engineering and Physical Sciences Research Council (EPSRC), grant number GR/S01481/01, and in part by the Swedish Foundation for International Cooperation in Research and Higher Education (STINT), contract IG2002-2049. Antti Kelloniemi has received funding from the Academy of Finland (project 201050) and the Nokia Foundation.

#### AUTHORS

**Damian T. Murphy** (dtm@ohm.york.ac.uk) received the B.Sc. (Hons) in mathematics in 1993; the M.Sc. in music technology in 1995; and the D.Phil. in music technology in 2000, all from the University of York, York, U.K. He is currently a lecturer in the Department of Electronics, University of York, and a visiting lecturer in the Department of Speech, Music and Hearing, KTH, Stockholm, Sweden. His research interests include physical modeling, spatial sound, and applications of the digital waveguide mesh. Dr Murphy is a member of the Audio Engineering Society.

**Antti Kelloniemi** (antti.kelloniemi@tkk.fi) received his M.Sc. from the University of Helsinki, Finland, in 2003. He is currently finalizing his doctoral thesis, "Room acoustics modeling with the digital waveguide mesh—Boundary structures and approximation methods," at the Helsinki University of Technology. He has recently been appointed as the technology manager for loudspeaker manufacturer Panphonics Oy, where his research concentrates mainly on electrostatic loudspeakers and active noise control. His interests include the modeling and design of acoustics and audio electronics.

**Jack Mullen** (jm220@ohm.york.ac.uk) received the M.Eng. in electronic engineering with music technology from the University of York, York, U.K., in 2002. His final year M.Eng. project involved research into digital waveguide mesh boundary implementations for room acoustics modeling. He has recently been awarded a Ph.D. degree from the University of York in 2006 for his thesis on multidimensional waveguide vocal-tract modeling. His research interests include speech and acoustical modeling.

**Simon Shelley** (sbs107@ohm.york.ac.uk) received the M.Eng. in electronic engineering with music technology systems from the University of York, U.K., in 2003. He is now working toward a Ph.D. on the accurate modeling of acoustic boundaries in the digital waveguide mesh, which is to be completed in 2007. Research interests include acoustic modeling, sound spatialization, and human-computer interaction for musical applications.

#### REFERENCES

- [1] S.A. Van Duyne and J.O. Smith, "Physical modeling with the 2-D Digital waveguide mesh," in *Proc. Int. Computer Music Conf.*, Tokyo, Japan, 1993, pp. 40–47.
- [2] V. Välimäki, J. Pakarinen, C. Erkut, and M. Karjalainen, "Discrete time modeling of music instruments," *Rep. Prog. Phys.*, vol. 69, pp. 1–78, Jan. 2006. [Online] Available: <http://www.iop.org/EJ/abstract/0034-4885/69/1/R01/>
- [3] S. Bilbao, *Wave and Scattering Methods for Numerical Simulation*. Chichester, UK: Wiley, 2004.
- [4] J.L. Kelly and C.C. Lochbaum, "Speech synthesis," in *Proc. Fourth Int. Congr. Acoustics*, Copenhagen, Denmark, Sept. 1962, pp. 1–4.
- [5] P.B. Johns and R.L. Buerle, "Numerical solution of 2-dimensional scattering problems using a transmission line matrix," *Proc. IEE*, vol. 118, pp. 1203–1208, Sept. 1971.
- [6] A. Fettweis, "Digital filters related to classical structures," *AEU: Archive für Elektronik und Übertragungstechnik*, vol. 25, pp. 78–89, Feb. 1971.
- [7] J.O. Smith, "A new approach to digital reverberation using closed waveguide networks," in *Proc. Int. Computer Music Conf.*, Vancouver, Canada, 1985, pp. 47–53.
- [8] J.O. Smith, "Music applications of digital waveguides," CCRMA, Stanford Univ., Stanford, CA, Tech. Rep. STAN-M-39, 1987.
- [9] J.O. Smith, "Physical modeling using digital waveguides," *Computer Music J.*, vol. 16, no. 4, pp. 74–87, 1992.
- [10] Stanford University News Service, "Music synthesis approaches sound quality of real instruments," Stanford University News Release, July 1994. [Online] Available: <http://www.stanford.edu/dept/news/pr/94/940607Arc4222.html>
- [11] J.O. Smith, "Principles of digital waveguide models of musical instruments," in *Applications of Digital Signal Processing to Audio and Acoustics*, M. Kahrs and K. Brandenburg, Eds. Boston, MA: Kluwer, pp. 417–466, 1998.
- [12] M. Karjalainen, P. Huang, and J.O. Smith, "Waveguide networks for room response modeling and synthesis," in *Proc. 118th AES Conv.*, Barcelona, Spain, preprint 6394, May 2005.
- [13] M. Karjalainen and C. Erkut, "Digital waveguides versus finite difference structures: Equivalence and mixed modeling," *EURASIP J. Applied Signal Processing*, vol. 7, pp. 978–989, June 2004.

- [14] C. Erku and M. Karjalainen, "Finite difference method vs. digital waveguide method in string instrument modeling and synthesis," in *Proc. ISMA 2003*, Mexico City, Dec. 2002.
- [15] A. Kelloniemi, "Frequency dependent boundary conditions for the 3-D digital waveguide mesh," in *Proc. 9th Int. Conf. Digital Audio Effects (DAFX06)*, Montréal, Canada, Sept. 2006, pp. 161-164. [Online]. Available: [http://www.dafx.ca/proceedings/papers/p\\_161.pdf](http://www.dafx.ca/proceedings/papers/p_161.pdf)
- [16] D.T. Murphy and M.J. Beeson, "The KW-boundary hybrid digital waveguide mesh for room acoustics applications," *IEEE Trans. Speech Audio Processing*, to be published.
- [17] M.J. Beeson and D.T. Murphy, "RoomWeaver: A digital waveguide mesh based room acoustics research tool," in *Proc. 7th Int. Conf. Digital Audio Effects (DAFX04)*, Naples, Italy, Oct. 2004, pp. 268-273. [Online]. Available: [http://dafx04.na.infn.it/WebProc/ProcP\\_268.pdf](http://dafx04.na.infn.it/WebProc/ProcP_268.pdf)
- [18] F. Fontana and D. Rocchesso, "Signal-theoretic characterization of waveguide mesh geometries for models of two-dimensional wave propagation in elastic media," *IEEE Trans. Speech Audio Processing*, vol. 9, no. 2, pp. 152-161, Feb. 2001.
- [19] F. Fontana and D. Rocchesso, "A new formulation of the 2-D waveguide mesh for percussion instruments," in *Proc. XI Colloq. Musical Informatics*, Bologna, Italy, Nov. pp. 27-30, 1995.
- [20] J. Laird, P. Masri, and N. Canagarajah, "Modeling diffusion at the boundary of a digital waveguide mesh," in *Proc. Int. Computer Music Conf.*, Beijing, China, Oct. 1999, pp. 492-495.
- [21] S.A. Van Duyne and J.O. Smith, "A simplified approach to modeling dispersion caused by stiffness in strings and plates," in *Proc. Int. Computer Music Conf.*, Aarhus, Denmark, 1994, pp. 407-410.
- [22] D.T. Murphy and D.M. Howard, "2-D digital waveguide mesh topologies in room acoustics modeling," in *Proc. 3rd Int. Conf. Digital Audio Effects (DAFX00)*, Verona, Italy, Dec. 2000, pp. 211-216 [Online]. Available: <http://profs.sci.univr.it/~dafx/DAFx-final-papers.html>
- [23] L. Savioja, T.J. Rinne, and T. Takala, "Simulation of room acoustics with a 3-D finite difference mesh," in *Proc. Int. Computer Music Conf.*, Aarhus, Denmark, 1994, pp. 463-466.
- [24] S.A. Van Duyne and J.O. Smith III, "The 3-D tetrahedral digital waveguide mesh with musical applications," in *Proc. Int. Computer Music Conf.*, Hong Kong, 1996, pp. 9-16.
- [25] S.J. Miklavcic and J. Ericsson, "Practical implementation of the 3D tetrahedral TLM method and visualization of room acoustics," in *Proc. 7th Int. Conf. Digital Audio Effects (DAFX-04)*, Naples, Italy, Oct. 2004, pp. 262-267. [Online]. Available: [http://dafx04.na.infn.it/WebProc/ProcP\\_262.pdf](http://dafx04.na.infn.it/WebProc/ProcP_262.pdf)
- [26] F. Fontana, D. Rocchesso, and E. Apollonio, "Using the waveguide mesh in modeling 3-D resonators," in *Proc. 3rd Int. Conf. Digital Audio Effects (DAFX-00)*, Verona, Italy, Dec. 2000, pp. 229-232 [Online]. Available: <http://profs.sci.univr.it/~dafx/DAFx-final-papers.html>
- [27] G.R. Campos and D.M. Howard, "On the computational efficiency of different waveguide mesh topologies for room acoustic simulation," *IEEE Trans. Speech Audio Processing*, vol. 13, no. 5, pp. 1063-1072, Sept. 2005.
- [28] M.L. Aird, J. Laird, and J. Ffitch, "Modeling a drum by interfacing 2-D and 3-D waveguide meshes," in *Proc. Int. Computer Music Conf.*, Berlin, Germany, Aug. 2000, pp. 82-85.
- [29] F. Fontana, "Physics-based models for the acoustic representation of space in virtual environments," Ph.D. dissertation, Dept. Computer Science, Univ. of Verona, Italy, Apr. 2003. [Online]. Available: <http://profs.sci.univr.it/~fontana/paper20.pdf>
- [30] D. Rossiter, A. Horner, and G. Baciu, "Visualization and manipulation of 3D digital waveguide structures," in *Proc. Int. Computer Music Conf.*, Beijing, China, 1999, pp. 43-46.
- [31] P. Huang, S. Serafin, and J.O. Smith, "A 3-D waveguide mesh model of high-frequency violin body resonances," in *Proc. Int. Computer Music Conf.*, Berlin, Germany, Aug. 2000, pp. 86-89.
- [32] S. Serafin, P. Huang, and J.O. Smith, "The banded digital waveguide mesh," in *Proc. MOSART Workshop Current Research Directions Computer Music*, Barcelona, Spain, Nov. 2001. [Online]. Available: <http://www.imi.aau.dk/~sts/publications/mosart.pdf>
- [33] A. Kelloniemi, V. Välimäki, and L. Savioja, "Simulation of room acoustics using 2-D digital waveguide meshes," in *Proc. IEEE Int. Conf. Acoustics, Speech, and Signal Processing (ICASSP)*, Toulouse, France, May 2006, pp. 313-316.
- [34] L. Savioja and V. Välimäki, "Reducing the dispersion error in the digital waveguide mesh using interpolation and frequency warping techniques," *IEEE Trans. Speech Audio Processing*, vol. 8, no. 2, pp. 184-194, Mar. 2000.
- [35] L. Savioja and V. Välimäki, "Interpolated rectangular 3-D digital waveguide mesh algorithms with frequency warping," *IEEE Trans. Speech Audio Processing*, vol. 11, no. 6, pp. 783-789, Nov. 2003.
- [36] F. Fontana and D. Rocchesso, "Online correction of dispersion in 2D waveguide meshes," in *Proc. Int. Computer Music Conf.*, Berlin, Germany, Aug. 2000, pp. 78-81.
- [37] F. Fontana, "Computation of linear filter networks containing delay-free loops, with an application to the waveguide mesh," *IEEE Trans. Speech Audio Processing*, vol. 11, no. 6, pp. 7743-782, Nov. 2003.
- [38] L. Savioja, T. Rinne, and T. Takala, "Simulation of room acoustics with a 3-D finite difference mesh," in *Proc. Int. Computer Music Conf.*, Aarhus, Denmark, Sept. 1994, pp. 463-466.
- [39] P.R. Cook, "Identification of control parameters in an articulatory vocal tract model with applications to the synthesis of singing," Ph.D. dissertation, Stanford Univ., Stanford, CA, 1990.
- [40] V. Välimäki and M. Karjalainen, "Improving the Kelly-Lochbaum vocal tract model using conical tube sections and fractional delay filtering techniques," in *Proc. Int. Conf. Spoken Language Processing (ICSLP)*, Yokohama, Japan, 1994, pp. 615-618.
- [41] S. Mathur and B.H. Story, "Vocal tract modeling: Implementation of continuous length variations in a half-sample delay Kelly-Lochbaum model," in *Proc. IEEE Intl. Symp. Signal Processing and Information Technology*, Darmstadt, Germany, 2003, pp. 753-756.
- [42] H.W. Strube, "Are conical segments useful for vocal-tract simulation?" *J. Acoust. Soc. Amer.*, vol. 114, no. 6, pp. 3028-3031, 2003.
- [43] J. Mullen, D.M. Howard, and D.T. Murphy, "Waveguide physical modeling of vocal tract acoustics: Flexible formant bandwidth control from increased model dimensionality," *IEEE Trans. Speech Audio Processing*, vol. 14, no. 3, pp. 964-971, May 2006.
- [44] J. Mullen, D.M. Howard, and D.T. Murphy, "Real-time dynamic articulations in the 2D waveguide mesh vocal tract model," *IEEE Trans. Speech Audio Processing*, submitted for publication, 2006.
- [45] B.H. Story, I.R. Titze, and E.A. Hoffman, "Vocal tract area functions from magnetic resonance imaging," *J. Acoust. Soc. Amer.*, vol. 100, no. 1, pp. 537-554, 1996.
- [46] D.G. Childers, *Speech Processing and Synthesis Toolboxes*. New York: Wiley, 2000.
- [47] J. Mullen, D.T. Murphy, and D.M. Howard, "Physical modeling of the vocal tract with the 2-D digital waveguide mesh," [Online]. Available: <http://www-users.york.ac.uk/~dtm3/vocaltract>
- [48] S. Shelley, "Acoustic modeling—The digital waveguide mesh," [Online]. Available: <http://www-users.york.ac.uk/~dtm3/vocaltract.html>
- [49] S.A. Van Duyne, J.R. Pierce, and J.O. Smith, "Traveling wave implementation of a lossless mode-coupling filter and the wave digital hammer," in *Proc. Int. Computer Music Conf.*, Aarhus, Denmark, 1994, pp. 411-418.
- [50] D. Rocchesso and F. Fontana, Eds., *The Sounding Object*. Florence, Italy: Mondo Estremo, 2003.
- [51] L. Savioja, J. Backman, A. Järvinen, and T. Takala, "Waveguide mesh method for low-frequency simulation of room acoustics," in *Proc. Int. Congr. Acoustics*, Trondheim, Norway, vol. 2, pp. 637-641, June 1995.
- [52] D.T. Murphy and M.J. Beeson, "Modeling spatial sound occlusion & diffraction effects with the digital waveguide mesh," in *Proc. Audio Eng. Soc. 24th Int. Conf.*, Banff, Canada, June 2003, pp. 207-216.
- [53] U. Stephenson, "Comparison of the image source method & the particle simulation method," *Appl. Acoust.*, vol. 29, no. 1, pp. 35-72, 1990.
- [54] A. Kelloniemi, V. Välimäki, and L. Savioja, "Simulation of room acoustics using 2-D digital waveguide meshes," in *Proc. IEEE Int. Conf. Acoustics, Speech, and Signal Processing (ICASSP)*, Toulouse, France, May 2006, pp. 163-168. [Online]. Available: [http://www2.hsu-hh.de/ant/dafx2002/papers/DAFX02\\_Murphy\\_Mullen\\_waveguide\\_mesh\\_modeling.pdf](http://www2.hsu-hh.de/ant/dafx2002/papers/DAFX02_Murphy_Mullen_waveguide_mesh_modeling.pdf)
- [55] A. Kelloniemi, D.T. Murphy, L. Savioja, and V. Välimäki, "Boundary conditions in a multi-dimensional digital waveguide mesh," in *Proc. IEEE Int. Conf. Acoustics, Speech, and Signal Processing (ICASSP)*, Montreal, Canada, May 2004, pp. IV-25-IV-28.
- [56] A. Kelloniemi, V. Välimäki, and L. Savioja, "Spatial filter-based absorbing boundary for the 2-D digital waveguide mesh," *IEEE Signal Processing Lett.*, vol. 12, no. 2, pp. 126-129, Feb. 2005.
- [57] A. Kelloniemi, "Improved adjustable boundary condition for the 3-D digital waveguide mesh," in *Proc. 2005 IEEE Workshop Applications of Signal Processing to Audio and Acoustics*, New Paltz, NY, Oct. 2005, pp. 191-194.
- [58] J. Huopaniemi, L. Savioja, and M. Karjalainen, "Modeling of reflections and air absorption in acoustical spaces: a digital filter design approach," in *Proc. 1997 IEEE Workshop Applications of Signal Processing to Audio and Acoustics*, New Paltz, NY, Oct. 1997.
- [59] K. Lee and J.O. Smith, "Implementation of a highly diffusing 2-D digital waveguide mesh with a quadratic residue diffuser," in *Proc. Int. Computer Music Conf.*, Miami, Florida, Nov. 2004. [Online]. Available: <http://ccrma.stanford.edu/~kglee/pubs/klee-icm04.pdf>
- [60] S. Shelley and D.T. Murphy, "Measuring diffusion in a 2-D digital waveguide mesh," in *Proc. 8th Int. Conf. Digital Audio Effects (DAFX-05)*, Madrid, Spain, Sept. 2005. [Online]. Available: [http://dafx05.ssr.upm.es/Proc\\_DAFX05/P\\_249.pdf](http://dafx05.ssr.upm.es/Proc_DAFX05/P_249.pdf)
- [61] D. Rocchesso and J.O. Smith, "Circulant and elliptic feedback delay networks for artificial reverberation," *IEEE Trans. Speech Audio Processing*, vol. 5, no. 1, pp. 51-63, Jan. 1997.
- [62] A. Kelloniemi, V. Välimäki, P. Huang, and L. Savioja, "Artificial reverberation using a hyper-dimensional FDTD mesh," in *Proc. 13th European Signal Processing Conf. (EUSIPCO 2005)*, Antalya, Turkey, Sept. 2005.
- [63] J. Merimaa, T. Lokki, T. Pelttonen, and M. Karjalainen, "Measurement, analysis, and visualization of directional room responses," presented at *AES 111th Conv.*, New York, NY, Nov. 2001, preprint 5449.